Hydrogenation and Disorder in Engineered Black TiO_2

Lei Liu,[1] Peter Y. Yu,[2] Xiaobo Chen,[3] Samuel S. Mao,[4,5] and D. Z. Shen[1]

[1]*State Key Laboratory of Luminescence and Applications, Changchun Institute of Optics, Fine Mechanics and Physics, Chinese Academy of Sciences, No. 3888 Dongnanhu Road, Changchun 130033, People's Republic of China*

[2]*Department of Physics, University of California at Berkeley, Berkeley, California 94720, USA*

[3]*University of Missouri-Kansas City, Department of Chemistry, Kansas City, Missouri 64110, USA*

[4]*Department of Mechanical Engineering, University of California at Berkeley, Berkeley, California 94720, USA*

[5]*Advanced Energy Technology Department, EETD, Lawrence Berkeley National Laboratory, Berkeley, California 94720, USA*

(Received 20 December 2012; revised manuscript received 25 March 2013; published 8 August 2013)

A new form of TiO_2 which is black in color has been shown to exhibit high efficiency for photocatalytic reactions under solar radiation [X. Chen, L. Liu, P. Y. Yu, and S. S. Mao, Science **331**, 746 (2011)]. However, the mechanism behind this disorder-engineering process is not fully understood. In this Letter, based on density functional theory, we describe the role of hydrogen in producing lattice disorder in the anatase nanocrystals. We clarify further that the highly localized nature of the midgap states results in spatial separation of photoexcited electrons and holes in black TiO_2, and that accounts for its high photocatalytic efficiency.

DOI: 10.1103/PhysRevLett.111.065505 PACS numbers: 61.72.−y, 61.46.−w, 68.47.Gh, 71.55.−i

Titanium dioxide (TiO_2) has been known as a good photocatalyst for water splitting since 1972 [1]. However, its band gap of more than 3.0 eV means that TiO_2 can absorb only the UV part of the solar spectrum, which accounts for about 5% of the solar radiation on Earth. Hence, the efficiency of TiO_2 for harvesting solar energy is rather low. This inefficiency of TiO_2 in photocatalytic water splitting originates from its electronic band structure. Although its conduction band minimum (CBM) matches the hydrogen electrode potential quite well, its valence band maximum (VBM) is about 1.6 eV below the oxidation potential [2] for water splitting. Because of this low-energy VBM, its absorption of the visible and near-infrared solar radiation is suppressed. Hence, in order to harvest solar energy more efficiently, it is necessary to "engineer" the TiO_2 band gap by raising its VBM energy so that its absorption onset matches better the electrolysis potential of 1.23 eV.

So far, many strategies have been proposed to reduce the band gap of TiO_2 to produce more efficient absorption of solar radiation. These approaches basically introduce impurities and/or defects [3–6] that produce midgap states. Impurities successfully doped into TiO_2 include metals [6,7]; nonmetallic elements such as C [8], N [9], S [10], and I [11]; and many others [2]. Through doping, the TiO_2 absorption in the visible has been increased but its overall photocatalytic efficiency remains insufficient to compete with other solar energy harvesting devices [3]. Recently, a large reduction (> 2 eV) in the TiO_2 band gap has been realized by hydrogenation of anatase nanocrystals under pressure [3]. This process results, for the first time, in a TiO_2 powder that is black in color [3]. In addition to a large absorption in the visible and infrared region, these "disorder-engineered" TiO_2 powders exhibit both high efficiency and stability in photocatalytic splitting of water [3,6] under solar irradiation.

By performing calculations based on the density functional theory (DFT) and the Perdew-Burke-Ernzerhof (PBE) functional, we have demonstrated that a disordered lattice containing O-H and Ti-H bonds can generate midgap states in TiO_2 and thereby shrink its absorption onset [3]. Recently, Lu *et al.* [12] have also shown by DFT-PBE calculations that the H adatoms on surface Ti_{5c} and O_{2c} atoms can induce lattice disorders and contribute to midgap states. However, to explain the formation of black TiO_2 via hydrogenation requires more than just the hydrogen termination of Ti and O dangling bonds on the anatase surface. A deeper understanding of the mechanisms responsible for the "disorder engineering" and resultant enhanced photocatalytic efficiency of hydrogenated TiO_2 is still lacking. For example, what exactly is the role of hydrogen in disordering the surface of the anatase nanocrystals? Normally, defects associated with disordered materials are detrimental to photocatalysis by acting as recombination sites [13,14]. Why did the disordered surface layer of black TiO_2 not quench its photocatalytic activities [13]? In this Letter, we have extended our DFT calculations to further clarify the physics behind the disorder engineering and high photocatalytic efficiency of black TiO_2.

Our DFT-PBE [15] calculations are performed using the projected augmented wave method as implemented by the Vienna *ab initio* simulation package (VASP) [16–19]. The hybrid functional [20] containing a mixture of the exact exchange (22%) and the PBE functional has been employed to correct the band gap problem of DFT in order to reproduce the experimental band gap value of 3.30 eV for anatase [3]. The cutoff energy for the plane-wave basis

set is 400 eV, and the Brillouin zone is sampled with a k-point separation smaller than 0.04 $Å^{-1}$. The experimental lattice parameters of anatase at room temperature ($a = 3.784$ Å, $c = 9.514$ Å) [21] are used in building structural models. Afterward, the atomic positions are relaxed until their residual forces are less than 0.005 eV $Å^{-1}$.

To understand how lattice disorder affects the anatase band structure, it is instructive to examine the dependence of its electronic energy bands upon lattice distortion. We start with a $2 \times 2 \times 1$ supercell with the formula $Ti_{16}O_{32}$ as shown in Fig. 1(a). We then distort the lattice by displacing either an O or a Ti atom from its starting equilibrium position with constrained geometry and analyze separately their effect on the band extrema. The displacements in both cases are selected to take place along the c axis [indicated by a green arrow in Fig. 1(a)], which has been shown, both experimentally and theoretically, to be the "softer" direction in the anatase phase [22]. The effects of distorting the two sublattices are quite different. As the O distortion is increased [shown in Fig. 1(b)], we find that the CBM does not change much while the VBM is blueshifted. For the Ti-sublattice distortions [shown in Fig. 1(c)], the CBM shows a redshift in addition to the blueshift of the VBM. The effects of the O distortion may be attributed to the fact that the CBM states arise mainly from the 3d orbitals of the sixfold-coordinated Ti atoms (denoted by Ti_{6c}) and are, therefore, insensitive to changes involving mainly the oxygen sublattice. However, during a displacement of the Ti sublattice, a shift of Ti_{6c} will deform six Ti-O bonds. This change will affect both the O-2p VBM and the Ti-3d CBM states. Moreover, since the Ti atoms are fixed with twice as many Ti-O bonds as the O atoms, it requires much more energy to deform the Ti sublattice than the O one by the same amount as shown in Figs. 1(b) and 1(c). This means that under the relatively low-energy process, the lattice disorder of anatase would be triggered mainly from the O sublattice. This result is consistent with the experimental observation that the band gap in black TiO_2 was reduced mainly from the large blueshift of VBM. However, although the O distortion in anatase can result in a large VBM blueshift, the distortion energy required to raise its VBM by ~2.18 eV as observed experimentally [3] is by far too high to be consistent with the experimental processing temperature of black TiO_2. It is necessary to consider the role of hydrogenation in reducing this energy for engineering the band gap.

We examined the hydrogenation effect by first considering the bulk anatase which was modeled again by the $2 \times 2 \times 1$ supercell in Fig. 2(a). The figure also shows the charge density distribution of its VBM electronic band, whose "dumbbell shape" distribution surrounding every O atom is characteristic of O 2p orbitals. After introducing an interstitial H_2 molecule into the supercell, we obtain model A as shown in Fig. 2(b). In Fig. 2(b), we plot the charge density distribution of the new highest-energy occupied band (HEOB) states, resulted from the bonding 1s orbitals of H_2 and the 2p orbitals of its neighboring O atoms. The hybridization between these orbitals makes the HEOB states behave like valence band states. Their energies calculated with the hybrid functional suggest that they are lying about 0.25 eV above the VBM of bulk anatase. In contrast, the CBM states in model A are extended over every Ti atom, as shown in Fig. 2(c). These charge distributions are almost identical to the typical $3d_{xy}$ orbitals. Thus, the itinerant nature of the conduction electrons has not been perturbed by the H_2 dopant. If the two H atoms in model A are separated and bonded to Ti and O atoms, respectively, then we obtain model B. We find that in model B a new midgap state whose energy is higher than the bulk VBM by 1.14 eV appears. This midgap state is also highly localized and composed of a mixture of the H_{1s}-Ti_{3d} bonding states and the 2p orbitals from the nearby O atoms, as shown

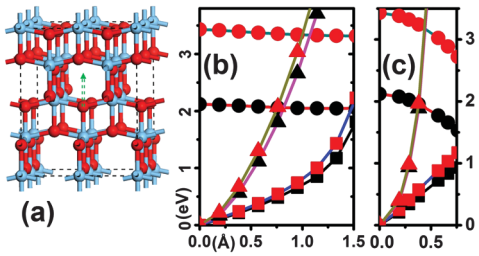

FIG. 1 (color). (a) $2 \times 2 \times 1$ anatase supercell, where the sky blue and red balls represent Ti and O atoms, respectively. The variations of VBM (represented by squares), CBM (circles), and total energy (triangles) calculated by PBE (colored in black) and by the hybrid functional (red) as a function of the distortion of (b) the O sublattice and (c) the Ti sublattice.

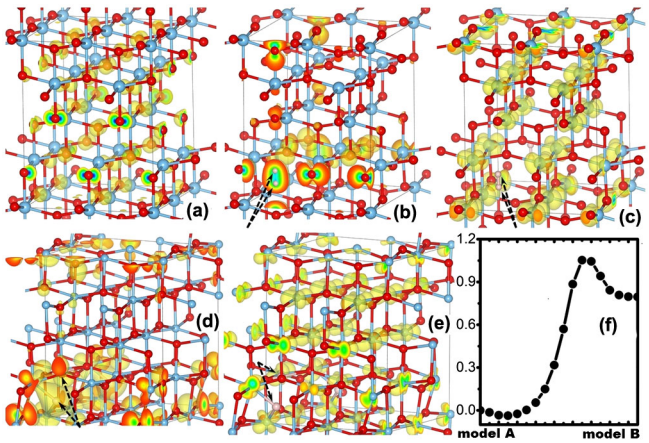

FIG. 2 (color online). Charge density distributions of the VBM band of (a) the $2 \times 2 \times 1$ anatase supercell, (b) the HEOB and (c) CBM bands of model A, (d) the midgap band and (e) the CBM band of model B, and (f) the minimum energy path from model A to model B. The locations of H atoms (represented by pink spheres) are highlighted by the black arrows.

in Fig. 2(d) (see the Supplemental Material [23]). In contrast, the electrons at the CBM band in model B, only 0.12 eV above the bulk CBM, are delocalized and their wave functions (mainly $3d$ character) are spread over all the Ti atoms, as shown in Fig. 2(e). Moreover, the alien Ti-O and H-O bonds also cause significant local lattice distortion. For example, the formation of Ti-H bonds pushes some neighboring O atom away by as much as 0.44 Å. Since both H bonding and lattice distortion can contribute to the changes of the electronic bands in model B, we have studied the effect of distortion alone by constructing another model: B', where the H atoms are removed from model B while keeping the lattice distortion unchanged. We find that the CBM electrons in model B' have about the same energies as in the bulk anatase, while its midgap state is now lowered to 0.55 eV above the bulk VBM.

The above results demonstrate again that the CBM electrons in anatase are neither very sensitive to local lattice distortions nor to changes induced by bonding to H. On the other hand, the midgap states above the bulk VBM respond to both lattice distortion and H bonding. The obvious conclusion is then that lattice distortions assisted by H bonding can be a good way to engineer the band gap of anatase, namely, by blueshifting its VBM while leaving the CBM more or less unchanged. In addition, the different spatial extent of the midgap hole states and the conduction electrons also suggests a spatial separation of the photoexcited electrons and holes leading to enhance photocatalytic efficiency. However, model B is not stable against decay into model A since it is 0.8 eV higher in energy than A. In Fig. 2(f), we show the minimum energy path from B to A calculated by the elastic band method. It indicates that there is an energy barrier of 0.25 eV for the lattice structure to go from model B to A. Hence, the H-assisted lattice distortion in bulk anatase is metastable. Even at room temperature, the lattice disorder will decay according to the process $(\sim\text{Ti-H}) + (\sim\text{O-H}) \Rightarrow (\sim\text{Ti-O}\sim) + \text{H}_2$.

Considering that surface atoms are less constrained and hence easier to reconstruct than the bulk ones, we have examined the hydrogenation process occurring at an anatase (001) surface [24,25]. In Fig. 3(a), a H_2 molecule is physisorbed on the anatase surface. This model will be regarded as the reference state with the total energy set equal to 0 eV. If the H_2 molecule is decomposed into two H atoms which passivate one twofold-coordinated O atom (O_{2c}) and one fivefold-coordinated Ti atom (Ti_{5c}), respectively [as shown in Fig. 3(b)], then the system requires an additional energy of 0.21 eV to form such H adatoms on the surface. On the other hand, if the two H atoms are bonded, instead, to a top O_{3c} and a lower Ti_{6c} atom of the Y-shaped Ti_3O unit highlighted in yellow in Fig. 3(a), then the result is that the Ti_3O unit will be transformed into Ti_2OH which looks more like the open V-shaped "string" shown in Fig. 3(c). Thus, hydrogenation opens one O-Ti bond of the Ti_3O unit by forming an O-H bond and changes the linkage between the O_{3c} atom and the remaining two Ti atoms. As the O_{3c} atom is displaced from its original position, the vacancy it creates is filled in by the second H atom, which forms Ti-H bonds with the neighboring Ti atoms. At this point, the total energy of the relaxed anatase surface increases by 0.81 eV. After that, it becomes easier to break a second Ti-O bond. For example, Fig. 3(d) shows the model where one of the Ti-O bonds in the Ti_2OH unit (shown by the dashed green line) is broken. The energy for that to occur is now reduced to 0.19 eV. This result suggests that H atoms play the role of "scissors," which makes it easier to untie the Ti_3O "knots." As hydrogenation goes deeper below the anatase surface, the lattice will become more open, making it easier for reconstruction to occur. While our results suggest that hydrogenation can generate the desirable lattice distortion on the surface of bulk anatase, nevertheless, it is still energetically difficult to break the strong Ti-O bonds. This is not surprising, considering how strong is the Ti-O bond (with bond energy of 6.87 eV [26]), and the formation energy of an oxygen vacancy in bulk anatase is computed to be 4.2 eV. In fact, the energy difference of 0.81 eV we computed between the two models in Figs. 3(a) and 3(c) is comparable to the result found by Di Valenti *et al.* [27] that N doping can reduce the oxygen vacancy formation energy in bulk anatase to around 0.6 eV.

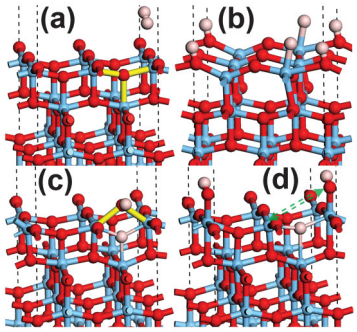

FIG. 3 (color). Relaxed anatase (001) surfaces with (a) a physisorbed H_2 molecule, (b) two H atoms bonded to top O_{2c} and Ti_{5c} atoms, respectively, (c) two H atoms bonded to O_{3c}, and (d) after a Ti_3O has been opened by two H atoms. The bonds of the Ti_3O "knot" to open are highlighted with yellow, and the broken bond of Ti_2OH is shown with a dashed line with a double arrow.

For the hydrogenation triggered lattice-disordering process to occur, a nanophase anatase has two advantages. First of all, it has a much bigger surface-to-bulk ratio over the bulk phase. Second, the surface atoms on nanocrystals (NCs) have more degrees of freedom to reconstruct than a bulk surface. To explore this low-dimensionality effect, we consider the hydrogenation of a 1 nm size NC of the formula of $Ti_{25}O_{50}$. As shown in Fig. 4(a), the dangling bonds of its four singly coordinated O atoms are passivated

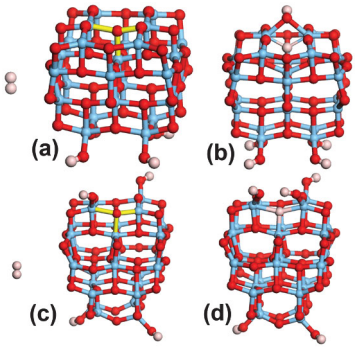

FIG. 4 (color). 1 nm anatase nanocrystal models: (a) $Ti_{25}O_{50}H_4$ with an isolated H_2 molecule, (b) $Ti_{25}O_{50}H_6$ with a Ti_3O unit opened up by H bondings, (c) $Ti_{29}O_{58}H_4$ with an isolated H_2 molecule, and (d) $Ti_{29}O_{58}H_6$ containing a Ti_3O unit opened up by H bondings.

with H atoms. In actual experiments, such H passivation will occur during the preparation of the anatase NC powder even before hydrogenation. Here, we assume again that an extra H_2 molecule is now added to break up the highlighted Ti_3O unit in Fig. 4(a). As in the case of the (001) bulk anatase surface, the Ti_3O "knot" is transformed, upon hydrogenation, into a Ti_2OH "string," while the second H atom replaces the central O_{3c} atom by forming Ti-H bonds, as shown in Fig. 4(b). However, unlike the (001) bulk anatase surface, the total energy for forming the Ti_2OH string in the 1 nm NC is *lowered* by 0.136 eV, compared to that of the configuration in Fig. 4(a). In other words, the breaking of Ti-O bonds has been transformed from being endothermic to exothermic as the sample size is decreased to nm dimensions. For another H-passivated NC model, named as "sc29" previously [28], shown in Fig. 4(c), it takes only 3.9 meV (equivalent to 45 K) to open all three Ti-O bonds in the Ti_3O knot, as shown in Fig. 4(d). This demonstrates clearly the role of the surfaces of anatase NCs in facilitating the breaking of Ti-O bonds upon hydrogenation. For simplicity, we will represent this process schematically as $(\sim\text{Ti-O}\sim) + H_2 \Rightarrow (\sim\text{Ti-H}) + (\sim\text{O-H})$. Combining our bulk and nanocrystal anatase results, it is plausible that hydrogenation helps to break up Ti-O bonds near the surface of nanocrystals, while the reverse process $(\sim\text{Ti-H}) + (\sim\text{O-H}) \Rightarrow (\sim\text{Ti-O}\sim) + H_2$ allows new Ti-O bonds to reform inside the interior of the nanocrystal (see the Supplemental Material [29]). The combination of these two processes will cause the surface layer of a nanocrystal to become disordered. We note that TiO_2 exists in nature as three polymorphs: anatase, rutile, and brookite. These three structures all consist of TiO_6 octahedra. They differ only in the ways these octahedra are linked together. For example, in anatase, the octahedra share only edges, while in rutile they share both edges and corners. The biggest Ti-O-Ti angle is equal to 156° in anatase, while this angle is reduced to 130.6° in rutile. Hence, a structure which starts out as anatase will end up containing some rutilelike and brookitelike arrangements after many cycles of randomly breaking and reforming of the Ti-O bonds. The interplay between these two processes may also explain the stability of black TiO_2 under repeated photocatalytic reactions in the splitting of water. When hydrogen produced during the splitting of water attempts to penetrate deeper into the core of the nanocrystal, the large barrier height between models *A* and *B* in bulk anatase will prevent it from breaking up the Ti-O bonds in the core region. As a result, the core will remain in the anatase phase.

The hydrogenation-induced-disordering mechanism proposed here explains some experimental details quite well. For example, the disorder-engineered TiO_2 nanocrystals were realized in anatase nanocrystals of diameter ~8–10 nm. The black TiO_2 nanoparticles obtained after hydrogenation have a highly disordered outer layer with a thickness of ~1 nm surrounding a crystalline anatase core [3]. We note that the highly localized nature of the midgap holes associated with disordered anatase can explain the high efficiency of black TiO_2 in the photocatalytic splitting of water in spite of the presence of a large amount of disorder. When trapped in the disordered shell of black TiO_2 nanoparticles, the spatial overlap between these localized holes and the itinerant conduction electrons, whose wave function can spread throughout both the core and shell regions, is greatly minimized. This increases the recombination time of the photoexcited electron-hole pairs. Furthermore, any photoexcited holes generated in the anatase core of black TiO_2 nanoparticles will be driven to the surface layers by the higher VBM energy of the disordered surface layer. Once trapped there, these holes will now react with water molecules more readily than when they are in the crystalline core.

In conclusion, the lattice disorder in black TiO_2 can originate from the hydrogenation that helps to break up Ti-O bonds on the surfaces of anatase nanocrystals by forming Ti-H and O-H bonds. In bulk anatase, the reverse process to release hydrogen molecules is energetically more favorable. The interplay between these two processes stabilizes a disordered shell of anatase nanoparticles. The surface lattice disorder can blueshift the VBM of anatase by introducing midgap states while leaving its CBM almost unchanged. The strong localization of the midgap holes to the disordered surface layers decreases their spatial overlap with the itinerant electrons. This charge separation of the photoexcited electron and hole pairs can explain why disorder-engineered black TiO_2 is a highly efficient photocatalyst for splitting water under solar radiation.

L. L. acknowledges the support of the National Natural Science Foundation of China (No. 11174273) and the 100 Talents Program of the Chinese Academy of Sciences. X. C. thanks the College of Arts and Sciences, University of Missouri-Kansas City; the University of Missouri Research Board; and Dow Kokam for their support.

[1] A. Fujishima and K. Honda, Nature (London) **238**, 37 (1972).
[2] Y. Gai, J. Li, S. S. Li, J. B. Xia, and S. H. Wei, Phys. Rev. Lett. **102**, 036402 (2009).
[3] X. B. Chen, L. Liu, P. Y. Yu, and S. S. Mao, Science **331**, 746 (2011).
[4] X. B. Chen and S. S. Mao, Chem. Rev. **107**, 2891 (2007).
[5] X. B. Chen, S. H. Shen, L. J. Guo, and S. S. Mao, Chem. Rev. **110**, 6503 (2010).
[6] X. B. Chen, C. Li, M. Grätzel, R. Kostecki, and S. S. Mao, Chem. Soc. Rev. **41**, 7909 (2012).
[7] W. Choi, A. Termin, and M. R. Hoffmann, J. Phys. Chem. **98**, 13 669 (1994).
[8] J. H. Park, S. Kim, and A. J. Bard, Nano Lett. **6**, 24 (2006).
[9] R. Asahi, T. Morikawa, T. Ohwaki, K. Aoki, and Y. Taga, Science **293**, 269 (2001).
[10] T. Umebayashi, T. Yamaki, H. Itoh, and K. Asai, Appl. Phys. Lett. **81**, 454 (2002).
[11] J. He, Q. Liu, Z. Sun, W. Yan, G. Zhang, Z. Qi, P. Xu, Z. Wu, and S. Wei, J. Phys. Chem. C **114**, 6035 (2010).
[12] J. B. Lu, Y. Dai, H. Jin, and B. B. Huang, Phys. Chem. Chem. Phys. **13**, 18 063 (2011).
[13] U. Diebold, Nat. Chem. **3**, 271 (2011).
[14] A. L. Linsebigler, G. Q. Lu, and J. T. Yates, Jr., Chem. Rev. **95**, 735 (1995).
[15] J. P. Perdew, K. Burke, and M. Ernzerhof, Phys. Rev. Lett. **77**, 3865 (1996).
[16] G. Kresse and J. Hafner, Phys. Rev. B **47**, 558 (1993).
[17] G. Kresse and J. Furthmüller, Comput. Mater. Sci. **6**, 15 (1996).
[18] G. Kresse and J. Furthmüller, Phys. Rev. B **54**, 11 169 (1996).
[19] G. Kresse and D. Joubert, Phys. Rev. B **59**, 1758 (1999).
[20] A. V. Krukau, O. A. Vydrov, A. F. Izmaylov, and G. E. Scuseria, J. Chem. Phys. **125**, 224106 (2006).
[21] M. Horn, C. F. Schwerdtfeger, and E. P. Meagher, Z. Kristallogr. Bd. **136**, 273 (1972).
[22] W.-J. Yin, S. Chen, J-H. Yang, X.-G. Gong, Y. Yan, and S.-H. Wei, Appl. Phys. Lett. **96**, 221901 (2010).
[23] See the Supplemental Material http://link.aps.org/supplemental/10.1103/PhysRevLett.111.065505 for the origin of the midgap states of models *A* and *B*, together with the bulk VBM and CBM states, which can be verified from their density of states.
[24] U. Diebold, Surf. Sci. Rep. **48**, 53 (2003).
[25] Here, we consider a periodic slab geometry to represent the anatase (001) surface, where the 2×2 supercell contains an atomic slab with seven Ti_4O_8 atomic layers with a clean surface and a vacuum region thicker than 13 Å.
[26] H.-P. Loock, B. Simard, S. Wallin, and C. Linton, J. Chem. Phys. **109**, 8980 (1998).
[27] C. Di Valentin, G. Pacchioni, A. Selloni, S. Livraghi, and E. Giamello, J. Phys. Chem. B **109**, 11 414 (2005).
[28] A. Iacomino, G. Cantele, D. Ninno, I. Marri, and S. Ossicini, Phys. Rev. B **78**, 075405 (2008).
[29] See the Supplemental Material http://link.aps.org/supplemental/10.1103/PhysRevLett.111.065505 for the energetics of the intercalated H_2 molecule in anatase.